

Differential roles of epigenetic changes and Foxp3 expression in regulatory T cell-specific transcriptional regulation

Hiromasa Morikawa^{a,b,1}, Naganari Ohkura^{a,1}, Alexis Vandenbon^c, Masayoshi Itoh^{d,e,f,2}, Sayaka Nagao-Sato^{d,2}, Hideya Kawaji^{d,e,f,2}, Timo Lassmann^{d,e,2}, Piero Carninci^{d,e,2}, Yoshihide Hayashizaki^{d,f,2}, Alistair R. R. Forrest^{d,e,2}, Daron M. Standley^c, Hiroshi Date^b, Shimon Sakaguchi^{a,g,3}, and the FANTOM Consortium⁴

Departments of ^aExperimental Immunology and ^cSystems Immunology, World Premier International Immunology Frontier Research Center, Osaka University, Suita 565-0871, Japan; ^bDepartment of Thoracic Surgery, Kyoto University, Kyoto 606-8507, Japan; ^dRIKEN Omics Science Center, Yokohama 230-0045, Japan; ^eRIKEN Center for Life Science Technologies, Division of Genomic Technologies, Yokohama, Kanagawa 230-0045, Japan; ^fRIKEN Preventive Medicine and Diagnosis Innovation Program, Wako, Saitama 351-0198, Japan; and ^gCore Research for Evolutional Science and Technology (CREST), Japan Science and Technology Agency, Tokyo 102-0075, Japan

Contributed by Shimon Sakaguchi, July 12, 2013 (sent for review March 22, 2013)

Naturally occurring regulatory T (Treg) cells, which specifically express the transcription factor forkhead box P3 (Foxp3), are engaged in the maintenance of immunological self-tolerance and homeostasis. By transcriptional start site cluster analysis, we assessed here how genome-wide patterns of DNA methylation or Foxp3 binding sites were associated with Treg-specific gene expression. We found that Treg-specific DNA hypomethylated regions were closely associated with Treg up-regulated transcriptional start site clusters, whereas Foxp3 binding regions had no significant correlation with either up- or down-regulated clusters in nonactivated Treg cells. However, in activated Treg cells, Foxp3 binding regions showed a strong correlation with down-regulated clusters. In accordance with these findings, the above two features of activation-dependent gene regulation in Treg cells tend to occur at different locations in the genome. The results collectively indicate that Treg-specific DNA hypomethylation is instrumental in gene up-regulation in steady state Treg cells, whereas Foxp3 down-regulates the expression of its target genes in activated Treg cells. Thus, the two events seem to play distinct but complementary roles in Treg-specific gene expression.

Naturally occurring CD25⁺CD4⁺ regulatory T (Treg) cells are actively engaged in the maintenance of immunological self-tolerance and homeostasis by suppressing aberrant or excessive immune responses harmful to the host (1). The transcription factor forkhead box P3 (Foxp3), which is specifically expressed in CD25⁺CD4⁺ Treg cells, plays crucial roles in Treg cell development and function (2–4). The essential role of Foxp3 is best illustrated by *Foxp3* gene mutations. Immune dysregulation, polyendocrinopathy, enteropathy, X-linked syndrome in humans and Scurfy mutant mice, both bearing *Foxp3* mutations, spontaneously develops severe autoimmunity and systemic inflammation because of developmental or functional failure of natural Treg cells (3, 5). In addition, ectopic expression of Foxp3 confers suppressive function on peripheral CD4⁺CD25[−] conventional T (Tconv) cells (2, 3). Foxp3 has, therefore, been considered as a master regulator of Treg cell function and a lineage-specification factor for their development.

Alteration of the epigenome is another important factor for establishing the Treg cell lineage. Epigenetic gene modifications, such as DNA methylation, histone modifications, and nucleosome positioning, are essential for controlling gene expression, particularly for the stabilization and fixation of a cell lineage (6–11). We have recently shown that proper development of Treg cells requires the establishment of Treg-specific DNA hypomethylation pattern (12). The process is independent of Foxp3 expression and necessary for Foxp3⁺ T cells to acquire Foxp3-independent gene expression, lineage stability, and full suppressive activity. However, it remains elusive how the two events, Foxp3 expression and epigenetic modification, contribute to Treg-specific gene expression.

In this report, we have assessed the effects of Treg-specific DNA hypomethylation on Treg-type transcriptional regulation and also analyzed possible differences between epigenome-dependent transcriptional regulation and Foxp3-dependent transcriptional regulation. We show that the role of each regulation is different depending on the state of Treg cell activation (i.e., the genes with Treg-specific DNA hypomethylation tend to be up-regulated in Treg cells in the steady state, whereas the genes with Foxp3 binding regions tend to be down-regulated in activated Treg cells). These results, together with our previous study (12), strongly support the concepts that Treg-specific transcriptional regulation requires the combination of Foxp3 induction and the installment of Treg-type DNA hypomethylation and that each event has a distinct role in the regulation. These findings contribute to our understanding of the molecular mechanisms by which specific transcriptional networks are established in natural Treg cells to determine and maintain their functions.

This work is part of the FANTOM5 (Functional Annotation of the Mammalian Genome 5) Project. Data downloads, genomic tools, and copublished manuscripts are summarized at <http://fantom.gsc.riken.jp/5/>.

Results

Transcriptional Start Site Clusters with Treg-Specific Expression. As a part of the FANTOM5 Project, we first obtained whole-gene expression and transcriptional start site (TSS) profiles of Treg cells by the cap analysis of gene expression (CAGE) with single-molecule sequencer Heliscope. CAGE tags are short-length nucleotide sequence tags that enable us to determine where transcription starts and obtain the whole-gene expression profile accurately, because the method is free from the biases, such as PCR amplification and sequence similarity, which are inherent in DNA microarray analyses. By mapping CAGE tags onto the mouse genome, we found 48,374 and 45,705 potential TSSs in CD25⁺CD4⁺ natural Treg cells and CD25[−]CD4⁺CD44^{low} Tconv cells, respectively (Fig. S1A). The TSS expression profiles were mostly similar between the BALB/c and C57BL/6 mouse strains

Author contributions: H.M., N.O., P.C., Y.H., A.R.R.F., D.M.S., H.D., S.S., and F.C. designed research; H.M., M.I., S.N.-S., and F.C. performed research; F.C. contributed new reagents/analytic tools; H.M., A.V., H.K., T.L., and F.C. analyzed data; and H.M., N.O., and S.S. wrote the paper.

The authors declare no conflict of interest.

Data deposition: The sequences reported in this paper have been deposited in the DNA Data Base in Japan, <http://www.ddbj.nig.ac.jp/> (accession nos. DRA000868, DRA000991, and DRA001028).

¹H.M. and N.O. contributed equally to this work.

²RIKEN Omics Science Center ceased to exist as of April 1, 2013, due to RIKEN reorganization.

³To whom correspondence should be addressed. E-mail: shimon@ifrec.osaka-u.ac.jp.

⁴A complete list of the FANTOM Consortium can be found in [Supporting Information](#).

This article contains supporting information online at www.pnas.org/lookup/suppl/doi:10.1073/pnas.1312717110/-DCSupplemental.

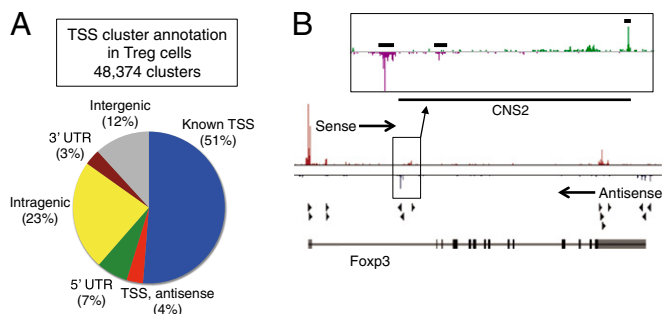


Fig. 1. TSS clusters identified in Treg cells. (A) Annotation of TSS clusters identified in Treg cells. (B) TSS clusters of the *Foxp3* locus. Upper and lower peaks show CAGE tags originating from the sense and antisense strands, respectively. Arrowheads indicate robust TSS clusters defined in the FANTOM5 work in ref. 40. Upper shows the magnification of the *Foxp3* CNS2 locus. TSS locations determined by FANTOM5 are indicated by horizontal lines.

(Fig. S1B). Many of them were located within the gene body regions, designated by National Center for Biotechnology Information (NCBI) RefSeq, in both Treg (Fig. 1A) and Tconv cells (Fig. S2A). In the *Foxp3* gene, for example, several potential TSSs were present within intron 1 and the last exon, and some of them were transcribed from its antisense strand (Fig. 1B). Interestingly, three TSS clusters were located on the *Foxp3* intron 1 region corresponding to the conserved noncoding sequence 2 (CNS2) region (13), suggesting that RNA polymerase II at CNS2 transcribed bidirectionally a unique class of enhancer RNAs as previously indicated (14). The potential TSSs identified in Treg or Tconv cells constituted only one-third of the TSSs found in all of the samples analyzed in FANTOM5, indicating that only a small portion of the genes was specifically expressed in Treg or Tconv cells (Fig. S1A). We also found that 23,583 TSSs were nonannotated TSSs by NCBI RefSeq; in particular, 336 nonannotated TSSs were specifically expressed in Treg cells. TSSs with opposite direction to their cognate gene TSSs were also frequently present in a variety of genes in accordance with the previous reports from FANTOM3 (15). In addition, TSS clusters expressed at significantly high levels were correlated with histone H3 lysine 4 trimethylation (H3K4me3) modification, a marker for euchromatin associated with transcriptionally permissive states, and nonexpressed TSS clusters with histone H3 lysine 27 trimethylation, a marker for heterochromatin associated with transcriptionally repressive states (Fig. S2B). These results indicate that the location of TSS clusters is tightly linked to a transcriptionally permissive state.

Among more than 45,000 TSS clusters, only 697 and 536 clusters were up- and down-regulated, respectively, in Treg cells compared with Tconv cells (Fig. 2A). Up-regulated genes include *Il2ra*, *Ctla4*, *Tnfrsf18*, and *Folr4*, which are so-called Treg signature genes (Table S1). To examine possible involvement of transcription factors in the differential expression, we analyzed transcription factor binding motifs in the -400 - to $+100$ -bp regions (promoter regions) from these differentially regulated

TSS clusters. Interestingly, motifs for Rel, NF- κ B, Tbp, and Irf4, which have been classified as T-cell receptor (TCR) stimulation-dependent transcriptional activators (16), were specifically enriched in the promoter regions of the Treg up-regulated TSS clusters (Fig. S2C), with a similar result (79% consistency) in C57BL/6 and BALB/c mice. Notably, whereas a large number of TSS clusters was up- or down-regulated in Tconv cells by TCR stimulation, down-regulated TSS clusters were dominant in Treg cells (Fig. 2B). In addition, although the number of up-regulated TSS clusters was higher in Tconv cells than Treg cells, more than one-half of the TSS clusters up-regulated in Treg cells were commonly up-regulated in Tconv cells (Fig. S2D), whereas 42.9% (172 of 401) were specifically up-regulated in Treg cells. Among down-regulated TSS clusters in Treg cells, 61.3% (1,814 of 2,955) were down-regulated in Tconv cells as well, whereas 38.7% (1,141 of 2,955) were down-regulated only in Treg cells.

We next performed transcription factor binding site analysis using overrepresentation index for the genes up- or down-regulated in Treg or Tconv cells by anti-CD3 and anti-CD28 antibody or phorbol 12-myristate 13-acetate/ionomycin treatment (Fig. S3), and we clustered the sets of genes according to the transcription factor binding site enrichment in their promoter regions (Fig. S4A). Significantly overrepresented motifs in the up- or down-regulated genes after stimulation were mostly shared between Treg and Tconv cells, irrespective of the ways of stimulation or mouse strains. This similarity indicates that stimulation-dependent gene expression in Treg and Tconv cells is controlled by similar transcription factors. In addition, those up-regulated TSS clusters in Treg and Tconv cells after TCR stimulation were prone to possess cytosine-phosphodiester-guanine (CpG) islands in their promoters (Fig. S4B).

Treg-Specific DNA Hypomethylation Pattern. We next analyzed the genome-wide DNA methylation status in Treg cells by methylated DNA immunoprecipitating sequencing (MeDIP-seq) (12). By analyzing the details of the whole DNA methylation pattern, we found that only 301 methylation peaks (0.19% of total peaks) showed Treg-dominant hypomethylation compared with Tconv cells (Fig. 3A). For example, a small region of the *Foxp3* intron 1 locus (corresponding to the CNS2 region) showed a differential DNA methylation pattern between Treg and Tconv cells, which was confirmed by bisulfite sequencing (Fig. 3B). The Treg-dominant hypomethylated regions were roughly 500 bp to 1 kbp long (Fig. 3C), and one-half of them were present within gene body regions, especially in intron 1 or 2 (Fig. 3A). Although a large portion of the differential peaks was also present in intergenic regions, the frequency of the peaks was very low compared with the frequency of the peaks in the gene body regions. In addition, differential peaks were rarely detected in CpG islands (Fig. 3A) or 5' upstream regions of TSSs (Fig. 4). Thus, differential DNA methylation is predominantly established in gene body regions, and the methylation status of promoters or CpG islands per se may not play a central role in Treg-specific transcriptional regulation. These observations are consistent with the previous reports showing that most differentially methylated regions were located in CpG-poor regions distal from annotated promoters (17).

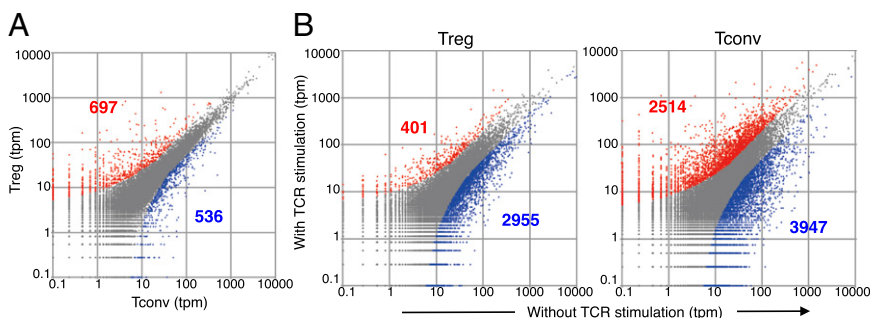


Fig. 2. Different transcriptional regulation between Treg and Tconv cells. (A) Comparison of TSS cluster expression between Tconv (x axis) and Treg (y axis) cells. Red and blue dots indicate significantly up- or down-regulated TSS clusters in Treg cells, respectively; tpm represents tags per million tags. (B) Significantly up- (red) or down-regulated (blue) TSS clusters after TCR stimulation in (Left) Treg or (Right) Tconv cells; x and y axes indicate TSS cluster expression before and after TCR stimulation, respectively.

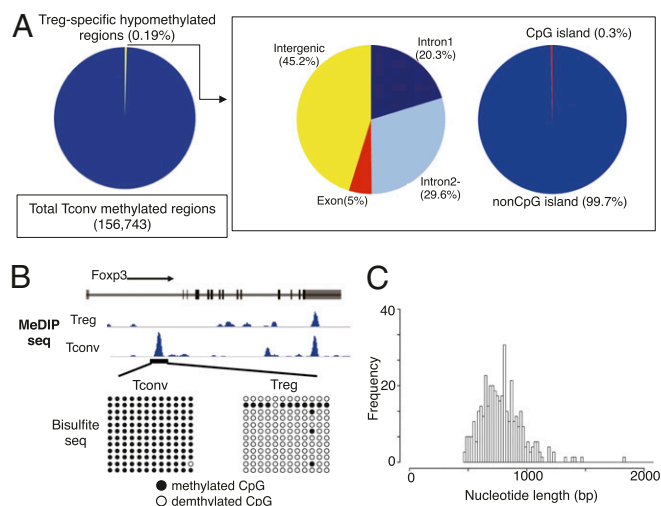


Fig. 3. Treg-specific DNA hypomethylated regions. (A) The ratio of TSDRs within total DNA methylation peaks of Tconv cells determined by MeDIP-seq and MACS. *Center* and *Right* show the annotation of TSDRs regarding location and association with CpG island. (B) DNA methylation pattern of the *Foxp3* locus by MeDIP-seq. Confirmations of the differences by bisulfite sequencing are shown below. Black and open circles indicate methylated and unmethylated CpG residues, respectively. Each column represents each CpG residue in the *Foxp3* CNS2 region. (C) Histogram of the length of TSDRs.

Correlation Between Treg-Specific TSS Clusters and Treg-Specific Hypomethylated Regions. To examine possible effects of Treg-specific DNA hypomethylation on Treg-type gene expression, we analyzed the relationship between the location of Treg-specific TSS clusters and the location of Treg-specific hypomethylated regions. TSS clusters located upstream of Treg-specific DNA demethylated regions (TSDRs) were prone to be up-regulated in Treg cells compared with Tconv cells, whereas TSS clusters downstream regions of TSDRs were rarely detected (Fig. 4). Interestingly, significant correlations existed between TSDRs and Treg-specific up-regulation of *Foxp3*-independent genes, such as *Ikzf2* and *Ikzf4* (18, 19). Statistical significance calculated based on hypergeometric distribution in the steady state was $P = 5.29 \times 10^{-11}$. The correlations were independent of TCR stimulation and the distance from TSS clusters to TSDRs. These results indicate that TSDRs within gene body regions may function as enhancer regions and thereby contribute to specific transcriptional regulation. In addition, DNA methylation status was inversely correlated

with the DNaseI hypersensitive regions (20) in 5' flanking regions of TSS clusters (Fig. S5A), indicating that DNA hypomethylated regions possess open chromatin structures that allow transcription factors to assemble on the regions. Thus, the DNA methylation status in Treg cells is fundamental for Treg-specific transcriptional regulation under both activated and nonactivated conditions.

We also examined possible involvement of transcription factors in hypomethylation-mediated Treg-specific gene expression, because differences in DNA methylation and histone modification status could determine the accessibility of transcription factors to specific gene loci (21). Search for enriched DNA sequence motifs within the Treg-specific hypomethylated regions revealed that motifs for Myb, Creb1, Irf5, Ets1, Arnt, Hif1a, Mfi2, Atf1, and Sp100 were significantly enriched in TSDRs compared with control genomic regions (Fig. S5C). Given that Ets1 and Creb1 bind to their target sites in a demethylation-dependent manner (7, 22), the results suggest that some of these transcription factors activate their target genes through direct binding to demethylated TSDRs.

Foxp3 Binding Regions in Treg Cells. Assuming that *Foxp3* is a lineage determination factor for Treg cells, we next examined how *Foxp3* contributed to the Treg-specific gene expression. *Foxp3* binding regions (20) were predominantly present in gene body regions, particularly around the TSSs. Transcription factor binding motifs for *Foxo3*, *Runx1*, *Irf4*, and *Ets1* were enriched within 500-bp regions from the *Foxp3* binding sites, which is consistent with the observation that *Foxp3* can associate with some of those transcription factors in Treg cells (Fig. S5D) (23).

The regions around the *Foxp3* binding sites tended to be demethylated and highly sensitive to DNaseI in both Treg and Tconv cells (Fig. 5), suggesting that the accessibility of the *Foxp3* binding sites is similar between Treg and Tconv cells. Likewise, the regions bound by *Ets1*, *Foxo1*, and *Elf1* in Treg cells showed similar profiles in DNaseI hypersensitivity and DNA hypomethylation status between Treg and Tconv cells (Fig. S5B). These results are in line with the previous report that enhancer landscape was mostly similar between Treg and Tconv cells (20, 24).

Respective Contributions of Treg-Specific DNA Hypomethylation and Foxp3 Expression to Treg-Specific TSS Clusters. Although the *Foxp3* binding regions are hypomethylated in general (Fig. 5), Treg-specific DNA hypomethylated regions and *Foxp3* binding regions were mostly different in Treg cells (Fig. 6A). To examine each contribution to the Treg-type gene expression, we compared the gene expression profiles of TSSs located on the adjacent regions of TSDRs or *Foxp3* binding sites.

First, to examine whether the contribution of TSDRs to Treg-specific gene regulation was independent of *Foxp3* expression, we

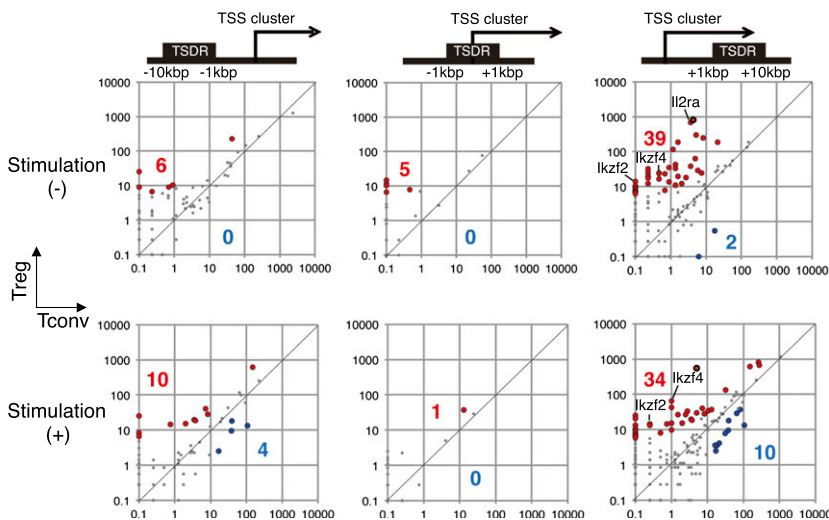


Fig. 4. Correlation of TSDRs with TSS clusters up-regulated in steady state Treg cells. Expression profiles of TSS clusters sorted by positional relation to TSDRs. Red and blue dots indicate significantly up- or down-regulated TSS clusters in Treg cells, respectively. *Upper* and *Lower* show expression profiles without and with TCR stimulation, respectively.

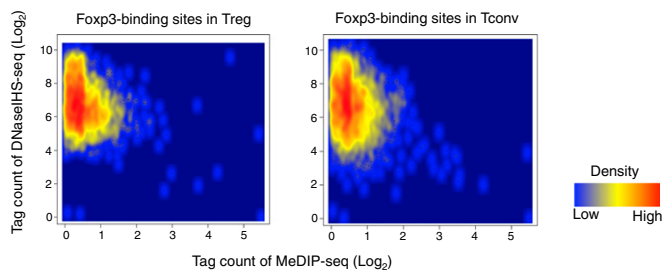


Fig. 5. Similarity in the chromatin status of Foxp3 binding sites. Heat maps show normalized tag counts of MeDIP-seq (x axis) and DNaseI-HS-seq (y axis) within 500 bp from Foxp3 binding sites of Treg cells in (Left) Treg and (Right) Tconv cells.

analyzed expression profiles of genes located within 10 kb of TSDRs in *Foxp3^{gfpko}* mice (20). In these mice, the insertion of GFP into the *Foxp3* locus marked Treg-committed cells, in which the *Foxp3* gene itself was disrupted. Clustering of microarray data revealed that a fraction of genes associated with Treg function was similarly regulated in both Foxp3-null Treg cells derived from *Foxp3^{gfpko}* mice and WT Treg cells (Fig. 6B). For example, *Ikzf2*, *Ikzf4*, and *Il2ra*, all of which were shown to be important for Treg-specific gene regulation and function (2–4, 19, 25), were commonly up-regulated in both. This Foxp3 independent up-regulation of specific genes indicates that a fraction of genes possessing TSDRs are controlled in a Treg-specific fashion without Foxp3.

Next, we analyzed the distribution of up- or down-regulated TSS clusters around TSDRs or Foxp3 binding sites in Treg cells. TSS clusters with TSDRs were highly enriched in the up-regulated TSS clusters in steady state Treg cells compared with

steady state Tconv cells. However, they did not show any significant enrichment in the up- or down-regulated TSS clusters in TCR-stimulated Treg cells (Fig. 6C). However, TSS clusters with Foxp3 binding sites were highly enriched in the down-regulated TSS clusters but not the up-regulated clusters in TCR-stimulated Treg cells (Fig. 6D). Notably, they were barely enriched in the up- or down-regulated TSS clusters in steady state Treg cells. One-half of the TSS clusters that were up-regulated in Tconv cells were not up-regulated in Treg cells after TCR stimulation, indicating that TCR stimulation-dependent up-regulation of genes was mostly inhibited in Foxp3-expressing Treg cells (Fig. S6A). In addition, calculation of cumulative distribution of up- or down-regulated TSS clusters around Foxp3 binding sites in Treg cells revealed that down-regulated clusters, but not up-regulated ones, tended to locate proximally to the Foxp3 binding sites (Fig. 6E and Fig. S6B). No such correlations were found with binding sites of other Treg-associated transcription factors, such as Ets1, Elf1, Foxo1, and Cbfb, in the distance between their binding sites and up- or down-regulated TSS clusters (Fig. S7).

Altogether, in Treg cells, TSDRs chiefly serve for up-regulation of gene expression in a steady state, whereas Foxp3 mainly engages in gene repression after TCR stimulation. Thus, TSDRs and Foxp3 seem to have distinct roles in the transcriptional regulation in Treg cells (Fig. 7).

Discussion

By addressing how Foxp3- and Treg-specific epigenome changes control Treg gene expression, we have shown in this report that Treg-specific TSS clusters located in the adjacent regions of TSDRs were mostly different from those TSS clusters in the Foxp3 binding regions. Moreover, transcription factor binding motifs found in TSDRs were different from those motifs in Foxp3 binding regions. These results strongly support the notion that Treg-specific DNA

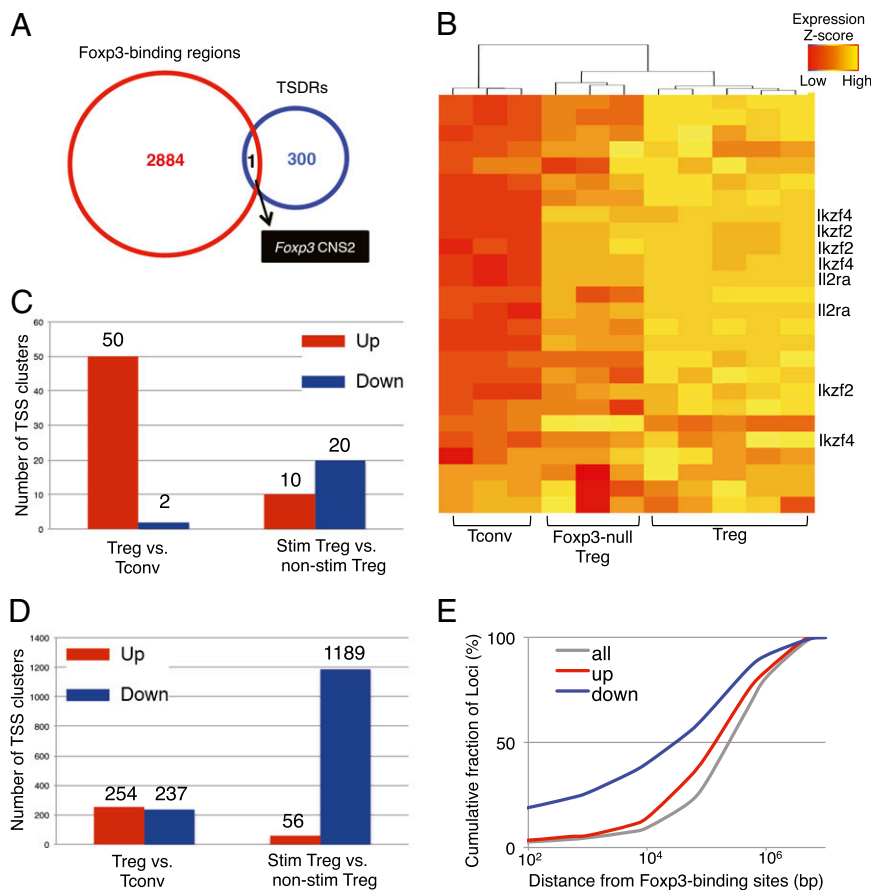


Fig. 6. TSDRs and Foxp3 distinctly contribute to Treg-specific gene regulation. (A) Venn diagram illustrating the lack of commonality between genomic regions of Foxp3 binding sites and TSDRs. (B) Gene expression profiles were compared among Tconv, Treg, and Foxp3-null Treg cells (20). Shown are the profiles of genes associated with TSS clusters that located within 10 kbp of TSDRs and showed up-regulation in Treg cells compared with Tconv cells. (C) Distribution of TSS clusters located within 10 kbp of TSDRs. (D) Distribution of TSS clusters locating within 10 kbp of Foxp3 binding sites. Samples of activated Treg cells were obtained from Treg cells stimulated with anti-CD3 and -CD28 antibodies for 6 h. (E) Cumulative distribution of TSS clusters within 1-Mbp regions from Foxp3 binding sites. Blue and red lines indicate TSS clusters significantly down- and up-regulated in Treg cells after TCR stimulation, respectively. Cumulative distribution of all TSS clusters is also shown as a negative control (gray line).

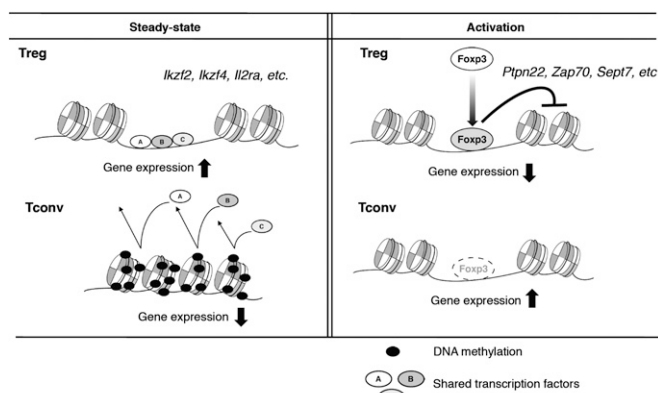


Fig. 7. Models of Treg-specific gene regulation by chromatin structures and transcription factors. Both chromatin structures and transcription factors coordinately regulate Treg-specific gene expression. Under the steady state, Treg-specific gene regulations are mainly dependent on chromatin structures specifically established in Treg cells. In contrast, under activated conditions, Foxp3 becomes functional and contributes to the gene regulation, especially to the repression of its target genes.

hypomethylation and Foxp3 expression play distinct but complementary roles in controlling Treg-specific gene expression and consequently, their function.

There are functional differences between Foxp3- and TSDR-dependent regulations in Treg-specific gene expression. TSS clusters possessing TSDRs were prone to be up-regulated in nonactivated Treg cells, whereas TSS clusters with Foxp3 binding sites tended to be down-regulated in activated Treg cells. These findings are in accord with the observation that suppressive function of Foxp3 is evident, especially after TCR stimulation (26, 27), and that DNA hypomethylation is linked to transcriptionally permissive states, which enable transcription factors to bind to their target gene loci (21). A recent study showed that active modification of the chromatin landscape was established during the course of Treg cell development and that Foxp3 contributed to the Treg function by exploiting the preexisting enhancer network (20). This finding is consistent with our observation that a limited number of gene loci was specifically demethylated in Treg cells and that the establishment of the DNA demethylation pattern was independent of Foxp3 expression (12). Thus, these findings collectively suggest that the installment of Treg-type DNA hypomethylation pattern is a prerequisite for establishing a preformed Treg-type enhancer network in Treg cells and that Foxp3 may function on the established enhancer landscape mainly as a gene repressor. This possible mechanism may explain Foxp3-independent expression of several Treg-specific genes (such as *Ikzf2* and *Ikzf4*), which seemed to be dependent on Treg-specific DNA hypomethylation, and the expression of several Treg signature genes in Foxp3-disrupted *Foxp3^{flpko}* mice, in which Treg-type DNA hypomethylation was installed (12, 18, 19, 28, 29).

In contrast with the notion discussed above, it was recently reported that Treg-type gene expression profiles could be established in Tconv cells by expressing a combination of Foxp3 and several other transcription factors (i.e., quintet transcription factors: Eos, IRF4, Satb1, Lef1, and GATA-1) (30). It suggests that the preexisting Treg-type enhancer landscape may not be essential for the recapitulation of Treg-type gene expression. One possible explanation is that the Treg-type DNA hypomethylation mainly contributes to the expression of several key transcription factors, including the quintet. In fact, TSDRs were found in the genes encoding *Ikzf4*, one of the quintet, as well as other key transcription factors for Treg cell function (12).

In the current study, we have identified 23,583 unannotated RNA transcripts in Treg cells, and some of them were specifically up-regulated in Treg cells in a TCR stimulation-independent manner. Many of the nonannotated TSS clusters are located in

intergenic regions, and some of those clusters located in gene body regions were antisense transcripts. These unannotated TSS clusters are also identified in human Treg cells, and some of them are confirmed to be splicing variants of Treg signature genes, such as *Foxp3* and *Ctla4*, by rapid amplification of cDNA ends PCR (31). Because intergenic regions and antisense strands of gene body regions are not to possess long ORFs, the majority of the nonannotated TSS clusters seems to be noncoding RNAs. As in the case of other cell types (32), noncoding RNAs up-regulated in Treg cells could play important roles in the development and function of Treg cells. Indeed, we found several species of antisense RNA transcripts from the *Foxp3* CNS2 region, which play a pivotal role in Foxp3 induction and its stability (13). Given that antisense RNA products function as a unique class of enhancer RNAs for their cognate gene expressions (14), it remains to be determined whether the unique RNA transcripts, such as antisense transcripts of CNS2, contribute to the establishment of Treg-type gene expression.

We found that several transcription factor binding motifs, such as motifs for Ets1 and Creb1, were frequent in Treg-specific DNA hypomethylated regions. It has been postulated that DNA methylation inhibits the recognition of DNA by some proteins (33, 34) and is generally associated with gene repression (35). In accordance with this notion, Ets1 binding to the *Foxp3* CNS2 region was only observed when CNS2 was demethylated (22). Creb/Atf was also shown to bind to the *Foxp3* CNS2 region in a demethylation-dependent manner (36). In addition, we found that H3K4me3 modification, indicating a transcriptionally permissive state, accumulated in the majority of promoters of expressed TSS clusters in Treg cells. This finding indicates that Treg-specific DNA demethylation together with other accompanied epigenetic modifications are required for specific gene expression by facilitating the binding of a variety of transcription factors to specific gene loci in Treg cells. The epigenetic changes would consequently lead to specific gene expression and the augmentation of its stability. However, in the adjacent regions of Foxp3 binding sites, different sets of binding motifs for transcription factors (Gabpa, Elk4, and Spi1) were frequently detected. Motifs for Foxo3 and Runx1, both of which were shown to associate with the Foxp3 protein in Treg cells (24, 37, 38), were also enriched in the Foxp3 binding regions. These observations collectively indicate that Foxp3 and its associating transcription factors are assembled on the preformed enhancer regions in an activation-dependent manner. Thus, TSDRs and Foxp3 seem to contribute distinctly to the Treg-type gene expression by using different sets of transcription factors.

In conclusion, the findings in this study suggest that, although functional transcription factors are mostly shared in Treg and Tconv cells, alteration of chromatin structures by Treg-specific epigenetic changes is important for up-regulating gene expression in Treg cells. In contrast, Foxp3 binding sites were highly correlated with transcriptional down-regulation in activated Treg cells, whereas they were mostly similar in chromatin status between Treg and Tconv cells. This finding suggests that Foxp3 becomes specifically expressed in developing Treg cells and subsequently binds, in an activation-dependent manner, to its target loci accessible in natural Treg cells and if ectopically expressed, Tconv cells (Fig. 7). This model explains the finding that Foxp3⁺ Treg cells can produce certain proinflammatory cytokines (such as IFN- γ) until they receive strong TCR stimulation, which shuts off the cytokine production and evokes potent suppressive activity through up-regulating suppression-associated molecules (39). The model can also be exploited to control a variety of physiological or pathological immune responses through peripheral generation of functionally stable Treg cells from conventional T cells and targeting the generation and functional stability of natural Treg cells.

Materials and Methods

Mice, Cell Sorting, and Cell Culture. C57BL/6 mice and BALB/c mice were purchased from CLEA Japan. CD4⁺ T cells were isolated from splenic and lymph nodes as previously described (2). CD4⁺CD25⁺ T cells (Treg cells) and CD4⁺CD25⁻CD44^{low} T cells (Tconv cells) were purified by sorting with a cell

sorter (MoFlo; Beckman Coulter). For in vitro TCR stimulation of Tconv cells, plates coated with anti-CD3 (1 μ g/mL) and anti-CD28 (1 μ g/mL) for 6 h or phorbol 12-myristate 13-acetate (20 ng/mL) and ionomycin (1 μ M) for 2 h were used.

Antibodies Used for Sorting and TCR Stimulation. Anti-IL2ra (PC61), anti-CD4 (RM4.5), anti-CD44 (IM7), anti-CD8a (53-6.7), anti-B220 (RA3-6B2), anti-CD16/32 (2.4G2), and anti-NK1.1 (PK136) were obtained from BD Pharmingen, Biolegend, or eBioscience. Anti-CD3 (2C11) and anti-CD28 (37.51) were used for in vitro T-cell stimulation. Mouse recombinant IL-2 was a gift from Shionogi Co.

RNA Preparation. Total RNAs for CAGE were extracted from sorted cells using miRNeasy Mini Kit (Qiagen).

CAGE Tag Expression Profiling. CAGE tag sequencings of each cell and sequence alignment to reference genome (mm9) were performed as a part of FANTOM5 (Fig. S8A) (40). Each TSS cluster expression level was calculated from normalized tag count at each robust TSS cluster defined in FANTOM5.

Processing of CAGE Data and Regulatory Motif Overrepresentation Analysis. Regions with differential levels of transcription initiation were defined based on the method described by Audic and Claverie (41). Overrepresentation index was calculated by the method described by Bajic et al. (42). Detailed methods are provided in *SI Materials and Methods*.

DNA Methylation Analysis. Raw MeDIP-seq data of Treg and Tconv cells were obtained from the study by Ohkura et al. (12). Sequence reads were mapped to the University of California Santa Cruz mouse genome mm9 using Bowtie program with default parameters (43). MACS (version 1.4) (44) was used to detect the specifically demethylated regions in Treg cells against Tconv cells

with the P value option = 1×10^{-15} as a cutoff for peak detection (Fig. S8 B–D). This stringent threshold was used to detect TSDRs like CNS2 in *Foxp3*.

ChIP-seq Data Analysis. Raw ChIP-seq data of H3K4me3 and histone H3 lysine 27 trimethylation histone modifications in mouse T cells (SRP000706) and raw ChIP-seq data of Ets1, Foxo1, Elf1, and Cbfb in mouse T cells (SRP015626) were obtained from the Short Read Archive Database (NCBI). DNaseI HS-seq data were obtained from the ENCODE repository. The tag data were mapped to the UCSC mouse genome mm9 using Bowtie (version 0.12.8) with default parameters. MACS (version 1.4) was used to identify the significant peaks of mapped data. The top 2,000 peaks were used as representative binding sites of each transcription factor in additional analysis. For analysis of *Foxp3*, 2,886 peaks reported by the previous report as its binding sites (20) were used. HOMER program (45) was used to calculate each ChIP-seq tag distribution at selected regions.

Data Access. The sequence tags of methylated DNA Immunoprecipitation and CAGE can be downloaded from the DNA Data Base in Japan, www.ddbj.nig.ac.jp/ (accession nos. DRA000868, DRA000991, and DRA001028).

ACKNOWLEDGMENTS. We thank R. Ishii for technical assistance, all members of the FANTOM5 Consortium for contributing to generation of samples and analysis of the dataset, and Genome Network Analysis Support Facility (GeNAS) for data production. This work was supported by Grants-in-Aid from the Japanese Ministry of Education, Culture, Sports, Science and Technology (MEXT) to the RIKEN Center for Life Science Technologies, to RIKEN Preventive Medicine and Diagnosis Innovation Program (to Y.H.), and to RIKEN Omics Science Center (to Y.H.); a grant of the Innovative Cell Biology by Innovative Technology (Cell Innovation Program) from MEXT (to Y.H.); and by Core Research for Evolutional Science and Technology (to S.S.) and Specially Promoted Research Grant-in-Aid 20002007 (to S.S.).

- Sakaguchi S, Yamaguchi T, Nomura T, Ono M (2008) Regulatory T cells and immune tolerance. *Cell* 133(5):775–787.
- Hori S, Nomura T, Sakaguchi S (2003) Control of regulatory T cell development by the transcription factor Foxp3. *Science* 299(5609):1057–1061.
- Fontenot JD, Gavin MA, Rudensky AY (2003) Foxp3 programs the development and function of CD4+CD25+ regulatory T cells. *Nat Immunol* 4(4):330–336.
- Khattry R, Cox T, Yasayko SA, Ramsdell F (2003) An essential role for Scurfin in CD4+CD25+ T regulatory cells. *Nat Immunol* 4(4):337–342.
- Bennett CL, et al. (2001) The immune dysregulation, polyendocrinopathy, enteropathy, X-linked syndrome (IPEX) is caused by mutations of FOXP3. *Nat Genet* 27(1):20–21.
- Musri MM, Párrizas M (2012) Epigenetic regulation of adipogenesis. *Curr Opin Clin Nutr Metab Care* 15(4):342–349.
- Kim JK, Samaranyake M, Pradhan S (2009) Epigenetic mechanisms in mammals. *Cell Mol Life Sci* 66(4):596–612.
- Jirtle RL, Skinner MK (2007) Environmental epigenomics and disease susceptibility. *Nat Rev Genet* 8(4):253–262.
- Waterland RA (2006) Epigenetic mechanisms and gastrointestinal development. *J Pediatr* 149(5, Suppl):S137–S142.
- Willingham AT, et al. (2005) A strategy for probing the function of noncoding RNAs finds a repressor of NFAT. *Science* 309(5740):1570–1573.
- Ashraf SI, Ip YT (1998) Transcriptional control: Repression by local chromatin modification. *Curr Biol* 8(19):R683–R686.
- Ohkura N, et al. (2012) T cell receptor stimulation-induced epigenetic changes and Foxp3 expression are independent and complementary events required for Treg cell development. *Immunity* 37(5):785–799.
- Zheng Y, et al. (2010) Role of conserved non-coding DNA elements in the Foxp3 gene in regulatory T-cell fate. *Nature* 463(7282):808–812.
- Ørom UA, et al. (2010) Long noncoding RNAs with enhancer-like function in human cells. *Cell* 143(1):46–58.
- Katayama S, et al. (2005) Antisense transcription in the mammalian transcriptome. *Science* 309(5740):1564–1566.
- Li Q, Verma IM (2002) NF-kappaB regulation in the immune system. *Nat Rev Immunol* 2(10):725–734.
- Schmid C, et al. (2009) Lineage-specific DNA methylation in T cells correlates with histone methylation and enhancer activity. *Genome Res* 19(7):1165–1174.
- Hill JA, et al. (2007) Foxp3 transcription-factor-dependent and -independent regulation of the regulatory T cell transcriptional signature. *Immunity* 27(5):786–800.
- Sugimoto N, et al. (2006) Foxp3-dependent and -independent molecules specific for CD25+CD4+ natural regulatory T cells revealed by DNA microarray analysis. *Int Immunol* 18(8):1197–1209.
- Samstein RM, et al. (2012) Foxp3 exploits a pre-existent enhancer landscape for regulatory T cell lineage specification. *Cell* 151(1):153–166.
- Thurman RE, et al. (2012) The accessible chromatin landscape of the human genome. *Nature* 489(7414):75–82.
- Polansky JK, et al. (2010) Methylation matters: Binding of Ets-1 to the demethylated Foxp3 gene contributes to the stabilization of Foxp3 expression in regulatory T cells. *J Mol Med (Berl)* 88(10):1029–1040.
- Rudra D, et al. (2012) Transcription factor Foxp3 and its protein partners form a complex regulatory network. *Nat Immunol* 13(10):1010–1019.
- Ono M, et al. (2007) Foxp3 controls regulatory T-cell function by interacting with AML1/Runx1. *Nature* 446(7136):685–689.
- Pan F, et al. (2009) Eos mediates Foxp3-dependent gene silencing in CD4+ regulatory T cells. *Science* 325(5944):1142–1146.
- Takahashi T, et al. (1998) Immunologic self-tolerance maintained by CD25+CD4+ naturally anergic and suppressive T cells: Induction of autoimmune disease by breaking their anergic/suppressive state. *Int Immunol* 10(12):1969–1980.
- Schubert LA, Jeffery E, Zhang Y, Ramsdell F, Ziegler SF (2001) Scurfin (FOXP3) acts as a repressor of transcription and regulates T cell activation. *J Biol Chem* 276(40):37672–37679.
- Gavin MA, et al. (2007) Foxp3-dependent programme of regulatory T-cell differentiation. *Nature* 445(7129):771–775.
- Lin W, et al. (2007) Regulatory T cell development in the absence of functional Foxp3. *Nat Immunol* 8(4):359–368.
- Fu W, et al. (2012) A multiply redundant genetic switch 'locks in' the transcriptional signature of regulatory T cells. *Nature Immunology* 13(10):972–980.
- Schmid C, et al. (2014) The enhancer and promoter landscape of human regulatory and conventional T cell subpopulations. *Blood*, 10.1182/blood-2013-02-486944.
- Guttman M, et al. (2011) lincRNAs act in the circuitry controlling pluripotency and differentiation. *Nature* 477(7364):295–300.
- Prokhorchouk E, Defossez PA (2008) The cell biology of DNA methylation in mammals. *Biochim Biophys Acta* 1783(11):2167–2173.
- Defossez PA, Stancheva I (2011) Biological functions of methyl-CpG-binding proteins. *Prog Mol Biol Transl Sci* 101:377–398.
- Weber M, Schübeler D (2007) Genomic patterns of DNA methylation: Targets and function of an epigenetic mark. *Curr Opin Cell Biol* 19(3):273–280.
- Kim HP, Leonard WJ (2007) CREB/ATF-dependent T cell receptor-induced FoxP3 gene expression: A role for DNA methylation. *J Exp Med* 204(7):1543–1551.
- Ouyang W, et al. (2010) Foxo proteins cooperatively control the differentiation of Foxp3+ regulatory T cells. *Nat Immunol* 11(7):618–627.
- Kerdiles YM, et al. (2010) Foxo transcription factors control regulatory T cell development and function. *Immunity* 33(6):890–904.
- Yamaguchi T, et al. (2013) Construction of self-recognizing regulatory T cells from conventional T cells by controlling CTLA-4 and IL-2 expression. *Proc Natl Acad Sci USA* 110(23):E2116–E2125.
- Forrest ARR, et al. (2014) A promoter level mammalian expression atlas. *Nature*, 10.1038/nature13182.
- Audic S, Claverie JM (1997) The significance of digital gene expression profiles. *Genome Res* 7(10):986–995.
- Bajic VB, Choudhary V, Hock CK (2004) Content analysis of the core promoter region of human genes. *In Silico Biol* 4(2):109–125.
- Langmead B, Trapnell C, Pop M, Salzberg SL (2009) Ultrafast and memory-efficient alignment of short DNA sequences to the human genome. *Genome Biol* 10(3):R25.
- Feng J, Liu T, Qin B, Zhang Y, Liu XS (2012) Identifying ChIP-seq enrichment using MACS. *Nat Protoc* 7(9):1728–1740.
- Heinz S, et al. (2010) Simple combinations of lineage-determining transcription factors prime cis-regulatory elements required for macrophage and B cell identities. *Mol Cell* 38(4):576–589.